

GERMANIUM DETECTOR FOR THE NEAR INFRARED

I. A. MCLAREN* and R. P. WAYNE

Physical Chemistry Laboratory, South Parks Road, Oxford OX1 3QZ (Gt. Britain)

(Received October 14, 1980)

Summary

In this work the construction and evaluation of a germanium detector for low level emission in the near-IR region (1.0 - 1.6 μm) are described. The noise equivalent power performance, for a device shaped to match the exit slit of a monochromator, was about $2 \times 10^{-14} \text{ W Hz}^{-1/2}$ at $\lambda = 1.40 \mu\text{m}$. Comparisons are given of the spectral and absolute responses for some alternative detectors.

1. Introduction

Several optical transitions of interest to the gas phase photochemist lie in the near-IR region, just beyond $\lambda = 1 \mu\text{m}$. For example, the maximum intensity of the highly forbidden $\text{O}_2(^1\Delta_g), v' = 0 \rightarrow \text{O}_2(^3\Sigma_g^-), v'' = 0$ band is at $\lambda = 1.269 \mu\text{m}$ [1], whilst the molecule HO_2 exhibits emission bands at $\lambda = 1.265 \mu\text{m}$ ($^2A', 001 \rightarrow ^2A'', 000$), $\lambda = 1.43 \mu\text{m}$ ($^2A', 000 \rightarrow ^2A'', 000$) and $\lambda = 1.51 \mu\text{m}$ ($^2A'', 200 \rightarrow ^2A'', 000$) [2, 3]. We have used these emissions to study the production of $\text{O}_2(^1\Delta_g)$ in ozone photolysis [4], the reaction [5] and quenching [6] of $\text{O}_2(^1\Delta_g)$, energy transfer between NO_2 and O_2 [7] and excitation and energy transfer in the HO_2 system [8, 9].

Early attempts by chemists [10, 11] to observe emission in this region involved photomultipliers with S1 cathodes (Ag-O-Cs) despite their large decrease in sensitivity below $\lambda = 1.0 \mu\text{m}$. Recent developments have produced an Ag-O-Cs photocathode with enhanced IR sensitivity, but the threshold is at a wavelength not much greater than $1.25 \mu\text{m}$ [12]. Semiconductor solid state devices can offer useful response well into the IR region, although they can suffer from excessive thermal noise if the band gap is too small, and they do not provide "noiseless" electron multiplication. Lead sulphide detectors have been used for some investigations of $\text{O}_2(^1\Delta_g)$ [13 - 15], although the effective sensitivity at $\lambda = 1.27 \mu\text{m}$ appears to have been no better than that of an S1 photomultiplier [15]. High sensitivity InSb [16] has superseded

*Present address: Centre de Recherches en Physique de l'Environnement, 45045 Orléans Cédex, France.

these devices, but again does not seem to be the ideal material for the spectral region around $1.27 \mu\text{m}$. A more suitable semiconductor material is germanium, which has a threshold wavelength corresponding to about $\lambda = 2 \mu\text{m}$. The first report of studies on $\text{O}_2(^1\Delta_g)$ using a germanium detector is that of Whitlow and Findlay [1] who employed a commercial photodiode (RCA Victor PD523). Our earlier emission studies were performed with intrinsic germanium photoconductors constructed in the laboratory [5, 11] and with a commercial photodiode [4, 7 - 9] (RCA type 6904A). In all cases the detector was cooled to liquid nitrogen temperature (77 K); these temperatures confer a large increase both in absolute sensitivity and in signal-to-noise ratio.

Contamination and damage sustained by our commercial photodiode during use for ten years led us to investigate in more detail the conditions yielding optimum sensitivity in the laboratory-constructed photoconductive detectors. We feel that other research groups may wish to make such detectors, since the preparation of the active element is relatively simple and the cost is very low. A particular advantage of the custom-built detector is that its geometry may be chosen to match that of the light source. The methods employed to make the detectors are described in this work and measurements of the relative spectral sensitivities and detection limits are presented. A comparison is given with two commercial devices.

2. Desired characteristics

Absolute sensitivity, in terms of output potential or current for a given intensity, is relatively unimportant so long as it is appreciably greater than the noise generated by any amplification stages used. As will appear later (Section 5), we employed preamplifiers cooled to 77 K. Experiments with dummy resistive sources showed that for all detectors tested the noise from the detector was at least ten times that from the amplifier. A more useful parameter than sensitivity is the noise equivalent power (NEP) which for our purpose may be defined as the root-mean-square (r.m.s.) value of radiant power falling on the detector that will give rise to an r.m.s. signal equal to the r.m.s. noise in a 1 Hz bandwidth. Thus, the smaller the NEP, the more satisfactory the device.

Since the detector material itself generates most of the noise, it is desirable that as much of the detector as possible should be "active". There are two consequences of this conclusion. First, the thickness of the detector is important. If the absorption occurs relatively near the surface of the germanium, then the remaining thickness acts only as a noisy shunt. Secondly, the entire surface area S of the detector should receive incident radiation. Because we wished to use our detectors with a small monochromator, we fashioned them in the form of strips of area approximately $5 \text{ mm} \times 2 \text{ mm}$ to match roughly the exit slit dimensions. In experiments where the detector has a large field of view, as for example where a detector-inter-

ference filter combination views a large test chamber, the requirement is that the ratio NEP/S should be as small as possible [17].

3. Fabrication of the germanium chip

The detectors were all prepared from a block of high purity germanium, kindly given by the Clarendon Laboratory, Oxford. This germanium is essentially intrinsic at room temperature. At 77 K the residual conduction makes it p type with less than 10^{14} charge carriers per cubic centimetre [18]. A slab of dimensions 2 mm \times 5 mm \times 6 mm was waxed onto a copper bar and slices were cut with a diamond-impregnated wire saw (oil lubricated). After cutting, the slice was waxed onto a stainless steel cylinder and was hand ground on water-lubricated grinding pads to remove all scratch marks on both surfaces. The detectors were then polished on flat slabs using 6 μ m and then 2 μ m diamond aerosol sprays and the thicknesses were measured. Finally, the detectors were cleaned by immersion in "533 White Etch" (5:3:2 HNO₃:HF:CH₃COOH).

Ohmic contacts were made to the germanium slices in an enclosed oven. A chip was placed on a sapphire disc mounted on a temperature-controlled heater and a piece of freshly cut indium (approximately 0.5 mm in diameter) was positioned at each end of the uppermost face. The oven was flushed with hydrogen and then with HCl-saturated hydrogen. The temperature was held first at 140 °C and then at 250 °C for 2 min. The hydrogen flow was stopped only when the temperature had dropped to 35 °C. Gold wire connections were soldered to the newly made contacts using indium solder.

A batch of five detectors was made, of which the thinnest (150 μ m) fractured while being mounted. The thicknesses of the remaining four were 245, 264, 376 and 512 μ m: these detectors are identified as D1, D2, D3 and D4 respectively.

4. Dewar vessel

Figure 1 shows the evacuable vessel used for mounting the detector and the preamplifier. In operation the inner chamber is filled with liquid nitrogen after the Dewar has been evacuated to below 10^{-5} Torr. A small slice of machinable glass is used to insulate the detector from the brass block, and two small posts in the block, to which the gold wires are soldered, allow the germanium to be held in contact by light spring action. Semiconductors for the preamplifiers are placed in holes drilled in the brass block, and other components are mounted close to the block.

5. Electrical behaviour of detectors

Several different liquid-nitrogen-cooled preamplifiers were used in the evaluation of our photoconductors and the commercial photodiodes. Figure

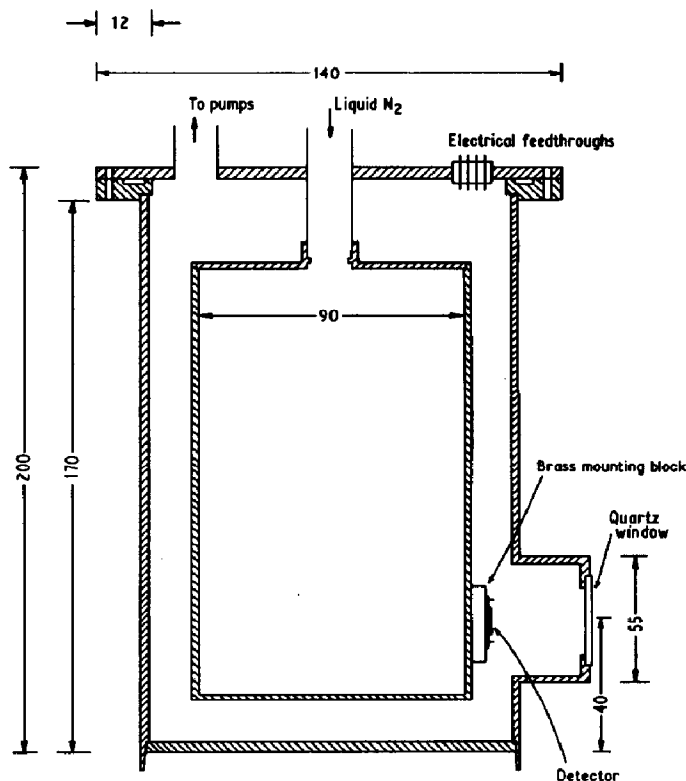


Fig. 1. A schematic diagram of the Dewar vessel. All dimensions are in millimetres.

2 shows the various configurations employed. Field effect transistors were used as the amplifying elements, since their characteristics do not change markedly at 77 K. Metal oxide film (2%) resistors were used throughout: the change in resistance between room temperature and 77 K was less than 5%.

The two commercial photodiodes tested (RCA type 6904A and Rofin type 7460) exhibit large resistances at 77 K in the reverse-biased condition. Source follower preamplifiers are therefore required. We decided to carry out initial testing of the photoconductive detectors using source followers. Circuit (a) was used to determine the response of the four detectors D1 - D4 as a function of bias current in the range 15 - 50 μA . A fixed intensity light source was passed through a monochromator (Section 6) and was chopped at 20 Hz. Figure 3 shows the results for $\lambda \approx 1.3 \mu\text{m}$. Since the curves must pass through the origin, the signal voltage developed does not increase linearly with increased bias current; the departure from linearity starts at lower currents with the thinner detectors. The custom-built photoconductors were bidirectional at room temperature. At 77 K they exhibited only very slight diode action at low currents. For example, the device D2 (264 μm thick) possessed resistances at 77 K of 408 $\text{k}\Omega$ and 453 $\text{k}\Omega$ with bias currents of 1 μA of opposite polarities. Both the diode behaviour and the resistance in each direction increased for bias currents in excess of about 10 μA . Currents were therefore subsequently kept below this level.

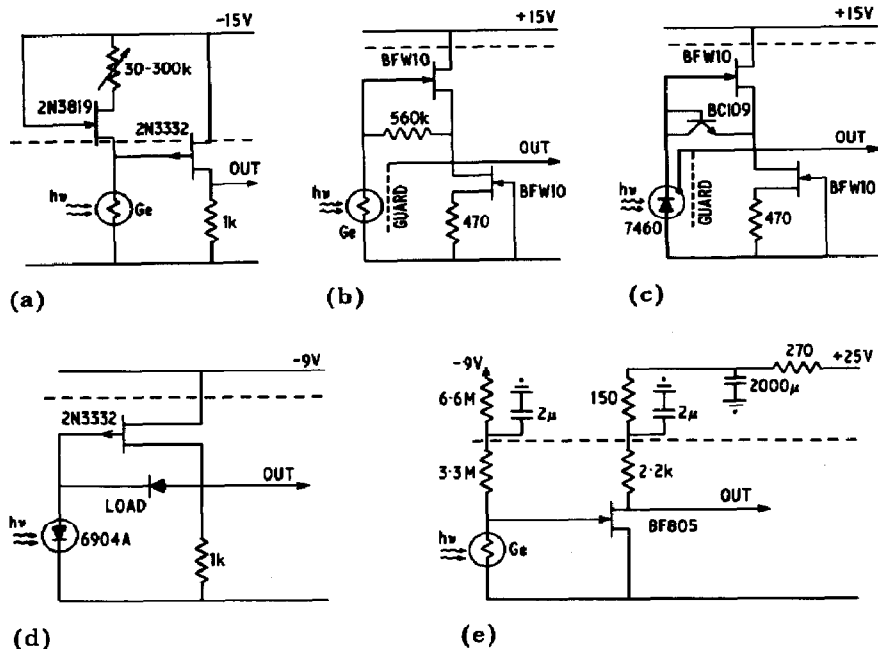


Fig. 2. Cooled preamplifier circuits (components below the broken lines are at 77 K): (a) variable bias current; (b), (c) low input capacitance; (d) RCA circuit [19]; (e) common source voltage amplifier.

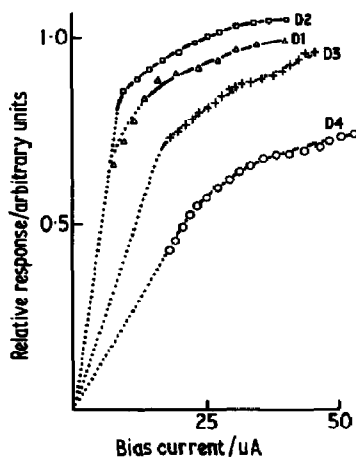


Fig. 3. Output voltage as a function of detector bias for a fixed light intensity (wavelength, $1.30 \pm 0.05 \mu\text{m}$; $\nu = 20 \text{ Hz}$): Δ , D1 ($245 \mu\text{m}$ thick); \square , D2 ($264 \mu\text{m}$ thick); $+$, D3 ($376 \mu\text{m}$ thick); \circ , D4 ($512 \mu\text{m}$ thick).

Circuits (b) - (d) provide low capacitive loading of the detector: in circuits (b) and (c) the amplifier output was also connected to a guard between the detector and the brass mounting block. The bias current in these circuits is determined only by the feedback load resistance and the gate-source potential at the operating transistor current. For the high resistance photodiodes a reverse-biased diode-connected silicon transistor

TABLE 1
Operating conditions and device characteristics

	<i>Detector</i>			
	<i>D2^a</i>	<i>D2^a</i>	<i>Rofin 7460</i>	<i>RCA 6904A</i>
Test circuit	(b)	(e)	(c)	(d)
Dark resistance at 77 K (Ω)	5.0×10^5	4.5×10^5	8×10^9	$\approx 10^9$ ^b
Load resistance (Ω)	5.6×10^5	3.3×10^6	1.2×10^{10}	10^9 ^c
Bias current (A)	6.6×10^{-6}	1.8×10^{-6}	3.1×10^{-10}	$\approx 2 \times 10^{-9}$ ^b
Rise or fall time (ms)	5	5	60	43 ^c
Transistor drain current (mA)	5.4	8.1	5.4	3.7

^aD2 is a photoconductive detector 264 μm thick.

^bEstimated from original operating conditions.

^cRCA data [19].

(circuit (c)) or silicon diode (circuit (d)) was used as load. Table 1 gives some operating conditions for the different circuits. It should be noted that the effective resistance of the various diode elements at 77 K appears to change with current, and the values given in the table refer to the specific bias currents.

Rise and fall times were measured with low intensity chopped radiation. At high intensities the response times became progressively shorter and the output waveform became more nearly square. The data given in Table 1 show that the turnover frequencies lie between a few hertz for the commercial photodiodes and about 45 Hz for the photoconductive detectors. This turnover frequency is important in relation to noise performance, since it seems that the major source of noise is "flicker" ($1/f$) in character. The chopping frequency ν is therefore limited. Beyond the turnover frequency the NEP is proportional to $\nu^{1/2}$, whereas at lower frequencies, ideally, it should be proportional to $1/\nu^{1/2}$. In our experiments we used a chopping frequency of 20 Hz, so that the photoconductive elements present an essentially resistive impedance. The experiments with circuits of types (b) and (c) make it clear that the frequency response is not limited by stray capacitances from the detector to ground or across the load. The d.c. resistances at 77 K for our photoconductors are approximately $5 \times 10^5 \Omega$, so that the effective capacitances are about 10^4 pF. Obviously, this is not the true terminal-to-terminal capacitance, and the frequency response must be determined by charge migration and recombination time in the semiconductor. At room temperature, where the equivalent source resistance is approximately 50 k Ω , there was no significant degradation of the square wave when chopping at 1 kHz, so that low temperature operation seems to be responsible for the relatively slow response. A similar effect is seen with the photodiodes, for which the low temperature effective capacitances are a few tens of picofarads. The manufacturers quote rise and fall times of 20 ns and 150 ns at room temperature, a factor of around 10^6 faster than the 77 K result; however, the reverse d.c. resistance is only reduced by a factor of around 10^4 .

The unimportance of stray capacitance in determining response times and the relatively low source impedance of the photoconductive detectors led us ultimately to adopt the common source preamplifier configuration (e). This circuit provides a voltage amplification of about ten times and alleviates problems of pick-up in connecting cables from the detector Dewar.

6. Optical performance

An optical train consisting of a stabilized incandescent lamp, a chopper (20 Hz), a monochromator and a detector was used to evaluate the performance of the detectors. The detector output was demodulated synchronously (Brookdeal model 9501D lock-in amplifier). The monochromator was a Bausch and Lomb model 33-86-25 with a -03 grating (a blaze of 675 lines mm^{-1} at $1.0 \mu\text{m}$; reciprocal linear dispersion, 12.8 nm mm^{-1}). Relative light intensities at the exit slit were measured as a function of wavelength with a Hewlett Packard model 8330 A radiant fluxmeter and a model 8334 A calibrated thermopile. Detector response was then determined at each wavelength (bandwidth (full width at half-maximum), approximately 2 nm; wavelength accuracy, $\pm 5 \text{ nm}$) and was normalized for the incident radiation intensity. Figure 4 (right-hand ordinate scale) shows the results for the

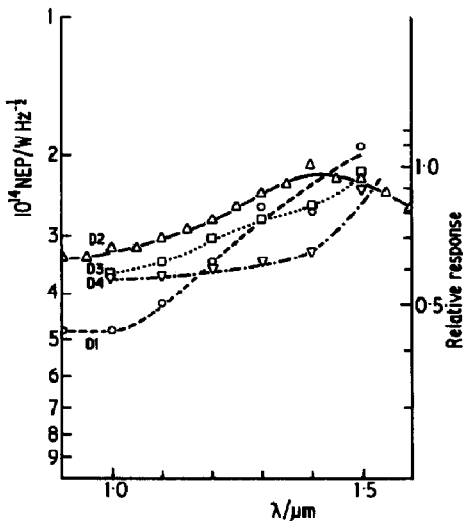


Fig. 4. Relative spectral response and absolute NEP as functions of wavelength for the four photoconductive detectors ($\nu = 20 \text{ Hz}$): \circ , D1; \triangle , D2; \square , D3; ∇ , D4.

detectors we constructed. Relative responses refer to the individual devices and require comparison with noise output to provide assessment of merit. An estimate of the absolute NEP was made in the following way. The thermopile detector was fixed behind the monochromator exit slits to present the same geometry as the detectors in the Dewar housing. The output intensity was determined at $\lambda = 1.40 \mu\text{m}$, the incident light was then attenuated by filters of measured transmission and the r.m.s. semiconductor output

was measured. R.m.s. (dark) noise in a 1 Hz bandwidth was very roughly obtained from chart recorder traces with a 1 Hz time constant in the demodulator filter. More sophisticated noise determinations require instruments not available to us.

Table 2 shows the results used in the calculation of NEPs of the D2 and Rofin model 7460 devices. For the other detectors the NEP was obtained by comparison of signal and noise measurements with those of the D2 detector subject to identical illumination. Figure 4 (left-hand ordinate scale) and Fig. 5 display NEP as a function of wavelength for the various detectors. As a result of the methods used for the determinations, particularly of r.m.s. noise, the NEP values are presented as estimates. However, the measurements do provide a clear basis for the selection of a device.

TABLE 2

Results used in estimating NEPs

	<i>Detector</i>	
	<i>D2</i>	<i>Rofin 7460</i>
Initial intensity at $\lambda = 1.40 \mu\text{m}$ ($\mu\text{W cm}^{-2}$)	2.4	26
Attenuator transmission	5.3×10^{-3}	2.2×10^{-4}
Detector area (cm^2)	10^{-1}	10^{-2} (estimate)
R.m.s. power on detector (μW)	6.4×10^{-4}	2.9×10^{-5}
R.m.s. signal (μV)	7.6×10^3	73
R.m.s. noise ($\mu\text{V Hz}^{-1/2}$)	0.25	4
Calculated NEP ($\text{W Hz}^{-1/2}$)	2.1×10^{-14}	1.6×10^{-12}

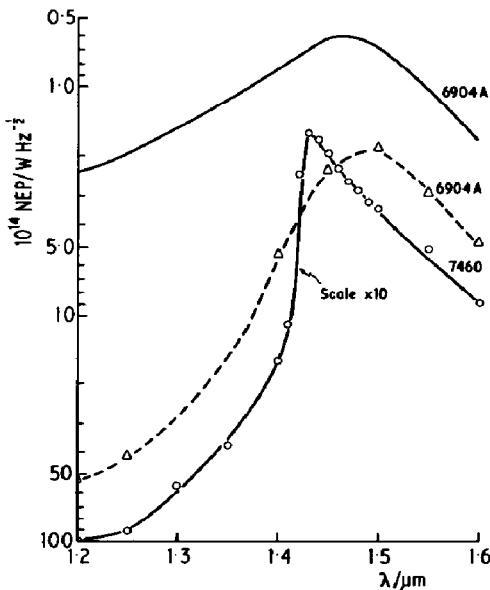


Fig. 5. NEP as a function of wavelength for the commercial photodiodes ($\nu = 20 \text{ Hz}$): Δ , RCA type 6904A; \circ , Rofin type 7460 (for this curve the values on the ordinate scale must be multiplied by ten); —, RCA type 6904A, manufacturer's data [19].

Figures 4 and 5 indicate that the NEP decreases as the wavelength increases up to 1.4 - 1.5 μm , and in general it increases again beyond that wavelength. The long-wavelength cut-off corresponds to the band gap in germanium (0.72 eV, corresponding to 1.70 μm at room temperature, and possibly 0.05 eV higher at 77 K [18]). The decrease in sensitivity towards shorter wavelengths probably results from increasing absorption of the incident radiation near the detector surface. In this connection the dramatic difference in spectral response at $\lambda < 1.40 \mu\text{m}$ between the photoconductors (Fig. 4) and photodiodes (Fig. 5) is noteworthy. With the diodes the radiation has to penetrate to the junction, whereas a region near the surface can be effective for the photoconductors. Photon absorption at $\lambda < 1.6 \mu\text{m}$ will be virtually complete within the first few microns from the surface [18]. The recombination thickness in the photoconductors might be orders of magnitude greater, which is why we fabricated detectors of different thicknesses. However, the four photoconductors show only relatively small differences in behaviour that can probably be ascribed to minor variations in surface conditions.

Comparison of the full and broken lines for the RCA type 6904A detector (Fig. 5) shows that the detector had indeed deteriorated in the ten years since it was tested by RCA [19]. Although at wavelengths greater than about 1.45 μm the NEP according to our estimate has increased by a factor of about 3, at shorter wavelengths the measured NEP increases much more rapidly than the specifications suggest. Thus, at $\lambda = 1.27 \mu\text{m}$, the wavelength of particular interest to us, the performance was some 20 times worse than intended. These results mean that for $\lambda = 1.27 \mu\text{m}$ the photoconductive detectors D1 - D4 are the most satisfactory of the devices tested.

For our chemical experiments [6] we selected the D2 device as having the smallest NEP at $\lambda = 1.27 \mu\text{m}$ (approximately $2.5 \times 10^{-14} \text{ W Hz}^{-1/2}$). The photon sensitivity corresponds to approximately $1.6 \times 10^5 \text{ photons s}^{-1}$ with a signal-to-noise ratio of unity and a bandwidth of 1 Hz. The Einstein A coefficient for the $\text{O}_2(^1\Delta_g \rightarrow ^3\Sigma_g^-)$ transition is about $2.6 \times 10^{-4} \text{ s}^{-1}$ at low pressures [20]. Direct viewing of a bulb 1 m in diameter through an interference filter (transmission, about 50%) might therefore allow optical detection of $\text{O}_2(^1\Delta_g)$ at concentrations around $10^9 \text{ molecules cm}^{-3}$ [17]. In practice we have used the monochromator and a flow tube having an observation region 56 mm in diameter. With this arrangement $[\text{O}_2(^1\Delta_g)]$ can be determined at concentrations of about $3 \times 10^{13} \text{ molecules cm}^{-3}$ at a signal-to-noise ratio of 100:1 (time constant, 1 s; monochromator bandpass, about 50 nm full width at half-maximum).

Acknowledgments

We should like to thank Professor R. A. Stradling and the Clarendon Laboratory, Oxford, for the kind provision of materials and facilities for the construction of the detectors. We wish to express our gratitude to both Professor Stradling and Mr. R. Cooke for the invaluable advice they gave us.

References

- 1 S. H. Whitlow and F. D. Findlay, *Can. J. Chem.*, **45** (1967) 2087.
- 2 K. H. Becker, E. H. Fink, P. Langen and U. Schurath, *Z. Naturforsch.*, **28a** (1973) 1872.
- 3 K. H. Becker, E. H. Fink, P. Langen and U. Schurath, *J. Chem. Phys.*, **60** (1974) 4623.
- 4 I. T. N. Jones and R. P. Wayne, *Proc. R. Soc. London, Ser. A*, **321** (1971) 409.
- 5 R. P. Wayne and J. N. Pitts, Jr., *J. Chem. Phys.*, **50** (1969) 3644.
- 6 I. A. McLaren, N. W. Morris and R. P. Wayne, *J. Photochem.*, in the press.
- 7 D. J. Giachardi, G. W. Harris and R. P. Wayne, *J. Chem. Soc., Faraday Trans. II*, **72** (1976) 619.
- 8 D. J. Giachardi, G. W. Harris and R. P. Wayne, *Chem. Phys. Lett.*, **32** (1975) 586.
- 9 J. R. Hislop and R. P. Wayne, *J. Chem. Soc., Faraday Trans. II*, **73** (1977) 506.
- 10 S. J. Arnold, R. J. Browne and E. A. Ogryzlo, *Photochem. Photobiol.*, **4** (1965) 963.
- 11 T. P. J. Izod and R. P. Wayne, *Nature (London)*, **217** (1968) 947.
- 12 M. Srinivasan, B. M. Blat and N. Govindarajan, *J. Phys. E*, **7** (1974) 859.
- 13 J. Noxon, *Can. J. Phys.*, **39** (1961) 1110.
- 14 A. Vallance-Jones and A. Harrison, *J. Atmos. Terr. Phys.*, **13** (1958) 45.
- 15 R. E. March, S. G. Furnival and H. I. Schiff, *Photochem. Photobiol.*, **4** (1965) 971.
- 16 D. N. B. Hall, R. S. Aikens, R. Joyce and T. W. McCurnin, *Appl. Opt.*, **14** (1975) 450.
- 17 R. H. Kummeler, *General Electric Company (Missile and Space Division) Rep. GE N-10875*, 1967.
- 18 R. J. Nicholas, personal communication, 1980.
- 19 E. J. Fjarlie, *RCA (Canada) Research Laboratories Rep. 96147-1*, 1969.
- 20 R. Badger, A. Wright and R. Whitlock, *J. Chem. Phys.*, **43** (1965) 4345.